Redox-Sensitive Microporous Membranes Prepared from Poly(vinylidene fluoride) Grafted with Viologen-Containing Polymer Side Chains

X. Liu, K. G. Neoh,* and E. T. Kang

Department of Chemical and Environmental Engineering, National University of Singapore, Kent Ridge, Singapore 119260

Received June 11, 2003; Revised Manuscript Received August 15, 2003

ABSTRACT: A viologen-containing microfiltration membrane (VBV-*g*-PVDF) was prepared from 4-vinylbenzyl chloride (VBC), poly(vinylidene fluoride) (PVDF), and 4,4′-bipyridine. The thermally induced graft copolymerization of VBC with ozone-preactivated PVDF was first carried out in *N*-methyl-2-pyrrolidone solution to produce VBC-*g*-PVDF copolymers. The resulting VBC-*g*-PVDF copolymers were cast into microfiltration membranes by phase inversion. Viologen was introduced by the reaction of 4,4′-bipyridine with VBC-*g*-PVDF membranes followed by diquaternization of the bipyridine via a second reaction with VBC. The resulting VBV-*g*-PVDF membranes were characterized using X-ray photoelectron spectroscopy, elemental analysis, scanning electron microscopy, and pore size distribution measurement. The VBV graft density has a profound effect on the structure and properties of the VBV-*g*-PVDF membranes. The permeability and flux of aqueous solutions through the membranes were investigated, and it was demonstrated that the viologen-containing membrane exhibited reversible permeability which can be regulated by redox reactions.

Introduction

At present, membrane processes are used in a wide range of applications such as reverse osmosis, electrodialysis, ultrafiltration, pervaporation, gas separation, hemodialysis, and controlled release of drugs.[1] Membrane science has also spread to the relatively new fields of enzyme electrodes, biosensors, and protein separation.[2−4] The most frequently used material for these applications is polymer membranes, which are chosen over inorganic membranes since polymers can be easily modified via chemical means. Poly(vinylidene fluoride) (PVDF) is one of the materials often used for microfiltration (MF) membranes (porous membranes containing fixed pores in the range 0.1−10 μm). However, because of the hydrophobic nature of the PVDF membranes, they have to be prewetted (e.g., by the use of ethanol) when used in aqueous media. A number of efforts including plasma treatment,[5,6] blending with hydrophilic polymers,[7] and ion beam irradiation[8] have been devoted to the chemical and physical modification of PVDF membranes to improve their surface biocompatibility and hydrophilicity, antifouling, pH-sensitive, and temperature-sensitive properties.[9−14] Redox-active polymers have also been introduced on membrane surfaces, and controllable reversible permeability and release of chemicals can be achieved.[15,16]

Surface coating or grafting monomers with different functional groups on existing membranes have been shown to be a convenient method to modify PVDF membranes.[12,17,18] For instance, through grafting of the acrylic acid polymer on the surfaces of membranes, hydrophilic and pH-sensitive properties have been successfully imparted to these membranes.[18,19] However, a surface coating may be easily removed, and the surface modification of existing membranes by grafting or graft copolymerization is likely to be accompanied by changes in membrane pore size and pore size distribution, leading to reduced permeability. In addition, the extents of grafting on the external membrane surface and on the surfaces of the pores may differ substantially. Thus, an alternative approach to membrane fabrication based on molecular or bulk graft copolymerization followed by phase inversion may prove to be particularly useful in facilitating the control of the composition of the pore surfaces through the control of the copolymer structure and composition.

In the present work, we report on the synthesis and characterization of PVDF with 4-vinylbenzyl chloride (VBC) polymer side chains introduced via the molecular graft copolymerization of VBC with ozone-preactivated PVDF in *N*-methyl-2-pyrrolidone (NMP) solution. The copolymer could be readily cast into MF membranes by the phase inversion technique. Viologen moieties were introduced by the subsequent Anderson reaction[20] between 4,4′-bipyridine and the VBC grafted PVDF membranes. Our interest in introducing viologen moieties in the membranes lies in their chemical stability and reversible conversions between two redox states. The existence of the viologen moieties in two different redox states allows the possibility of redox regulation of the membrane's permeability.[21] Since the amount of viologen moieties grafted can be expected to affect the membrane's structure and permeability, the issues of controlling the graft concentration and the subsequent effects on the membrane's properties were addressed.

Experimental Section

Materials. Poly(vinylidine fluoride), PVDF (Kynar, K-761), powder with molecular weight of 441 000 was obtained from Elf Atochem of North America Inc. 4-Vinylbenzyl chloride (VBC), 4,4′-bipyridine, 4-styrenesulfonic acid sodium salt hydrate ($H_2C{=}CHC_6H_4SO_3Na{\cdot}xH_2O$, SSA), ammonium cerium(IV) nitrate ($(NH_4)_2Ce(NO_3)_6$), and sodium hydrosulfite ($Na_2S_2O_4$) were obtained from Aldrich Chemical Co. NMP (reagent grade) was obtained from Merck Chemical Co. Other solvents and chemicals were of reagent grade and used as received from Aldrich Chemical Co.

Preparation of Viologen-Containing MF Membranes (Scheme 1). The PVDF powders were first dissolved in NMP to achieve a concentration of 7 wt %. A continuous stream of

* To whom correspondence should be addressed: Tel +65 68742186; Fax +65 67791936; e-mail chenkg@nus.edu.sg.

10.1021/ma034794o CCC: $25.00
Published on Web 10/16/2003

Scheme 1

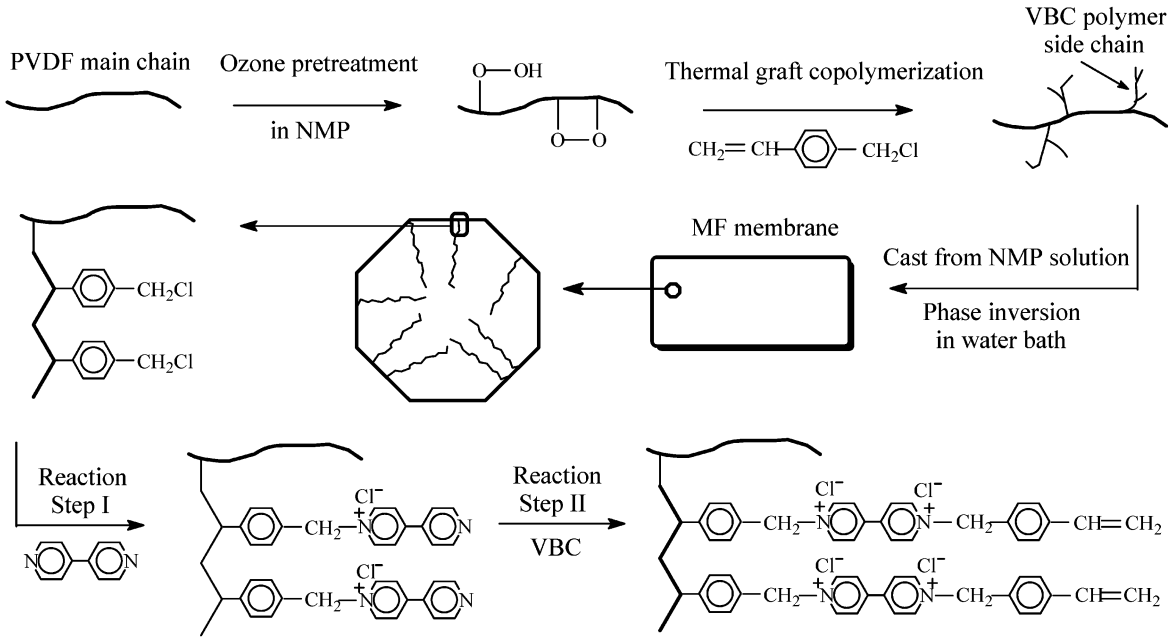

O_3/O_2 mixture (generated from an Azcozon RMU16-4-EM ozone generator) was bubbled through 30 mL of the PVDF/NMP solution at room temperature. The gas flow rate was adjusted to 300 L/h to give rise to an ozone concentration of about 0.027 g/L of the gas mixture. A treatment time of 15 min was used to achieve the desired content of peroxides in the PVDF chains since excessive ozone pretreatment will lead to the overoxidation and degradation of the polymer chains.[22] After the ozone preactivation, the polymer solution was cooled in an ice bath. Argon gas was introduced for about 30 min to remove the dissolved ozone and oxygen. The VBC monomer was then added to achieve a specific [VBC]/[$-CH_2CF_2-$] molar feed ratio. After an additional 15 min of argon purging, the mixture was heated at 60 °C to induce the decomposition of peroxide groups in the PVDF chains and to initiate the graft copolymerization of VBC for 4 h under a constant flow of argon. After the reaction, the resultant VBC-*g*-PVDF copolymer was precipitated in an excess amount of absolute (99.9%) ethanol (which is a good solvent for VBC). The copolymer was washed with ether (which is one of the solvents for VBC homopolymer and a nonsolvent for PVDF) and ethanol alternately for three cycles and then dried under vacuum before being subjected to subsequent characterization and reaction.

MF membranes were prepared by phase inversion from a NMP solution containing 10 wt % PVDF or VBC-*g*-PVDF copolymer at room temperature. The polymer or copolymer solution was cast onto a glass plate, which was then immersed in a bath of doubly distilled water (nonsolvent) after the polymer solution had been subjected to a brief period of evaporation (~10 s) in air. Each membrane was left in the water for about 20 min after its separation from the glass plate. The surface in contact with the glass plate is denoted as the "bottom surface", while the outer surface will be denoted as the "top surface" in the following sections. The membranes were put into an excess amount of doubly distilled water under constant stirring at room temperature for 24 h. The purified membranes were then dried under reduced pressure for subsequent characterization and will be denoted as the VBC-*g*-PVDF membranes.

Viologen moieties were introduced on the VBC-*g*-PVDF membranes by a two-step reaction. The VBC-*g*-PVDF membrane (about 0.03 g) was first reacted with 1.0 g of 4,4′-bipyridine (reaction step I in Scheme 1) in 15 mL of ethanol at 60 °C for 12 h. After the reaction, the yellowish membrane was washed with ethanol and then reacted with 1 mL of VBC in 15 mL of ethanol at 60 °C for another 12 h (reaction step II in Scheme 1). Excess 4,4′-bipyridine and VBC were used in reaction steps I and II to ensure complete reaction of the grafted VBC and diquaternization of the 4,4′-bipyridine. The resulting pale yellow vinylbenzyl viologen (VBV) grafted membrane (after reaction steps I and II) will be denoted as the VBV-*g*-PVDF membranes in the following sections. In Scheme 1, the VBC terminal groups are shown as the vinyl groups. It has to be recognized that the presence of the double bond can also lead to some degree of cross-linking between the viologen polymer side chains.

Tests and Characterization. Bulk C, H, and N analyses of the membranes were carried out on a Perkin-Elmer 2400 elemental analyzer while the F contents were determined by the Schöniger combustion method.[23] The surface composition was monitored by X-ray photoelectron spectroscopy (XPS) on a Kratos AXIS HSi spectrometer with a monochromatized Al Kα X-ray source at a constant dwell time of 100 ms and a pass energy of 40 eV. The core-level signals were obtained at a photoelectron takeoff angle (with respect to the sample surface) of 90°. In peak synthesis, the full width at half-maximum of the Gaussian peaks was maintained constant for all components in a particular spectrum. Surface elemental stoichiometries were determined from peak area ratios, after correcting with the experimentally determined sensitivity factors, and were reliable to ±5%.

The surface morphology of the MF membranes was investigated using a JEOL 6320 scanning electron microscope (SEM). A thin layer of platinum was sputtered onto the membrane surface for imaging purposes. The pore sizes of the pristine PVDF and the VBV-*g*-PVDF membrane were measured using a Coulter Porometer II apparatus, manufactured by Coulter Electronics Ltd., U.K. The commercial product, Porofil, for the Coulter Porometer instrument was used as a wetting agent. For each pore size value reported, at least three measurements were averaged.

The redox-sensitive permeation of the viologen-modified membranes was studied using SSA (which has an absorbance peak at 255 nm) as the permeant. The experimental setup used for studying the transport of SSA is shown schematically in Figure 1. Two milliliters of 10^{-2} M SSA solution was used in the glass cell, and the effective membrane area for transport was 0.5 cm^2. Before the permeation experiment, special care was taken to prevent leaks from the edges of the membrane. For the permeation test, the cell was immersed in a beaker containing 20 mL of doubly distilled water under a constant stirring rate of 300 rpm. The permeability of the membranes to SSA was assessed from the increase in the absorbance at 255 nm (measured using a Shimadzu UV-1601 PC scanning

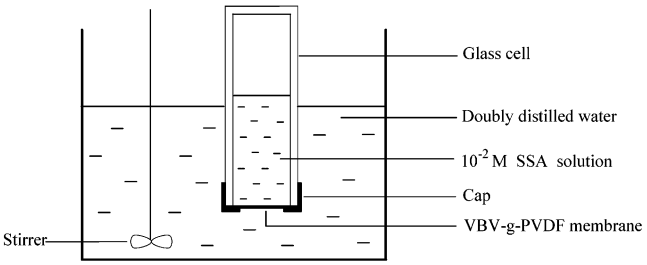

Figure 1. Experimental setup used for permeability study of VBV-*g*-PVDF membrane.

spectrophotometer) of the outer aqueous phase. To change the redox state of the viologen moieties on the membrane, the membrane was immersed in one of the redox agents, 0.1 M $Na_2S_2O_4$ (reducing) or 0.01 M $(NH_4)_2Ce(NO_3)_6$ (oxidizing), for 1 min. The exterior of the cell was rinsed with doubly distilled water to remove all traces of the reducing/oxidizing agent before commencing the permeation test. The presence of the oxidizing/reducing agent in the membrane pores is not expected to interfere with the absorbance measurements since both the oxidizing and reducing agents do not absorb at 255 nm. The experiment was repeated several cycles with the membrane alternately being dipped in $Na_2S_2O_4$ or $(NH_4)_2Ce(NO_3)_6$ to change the viologen's redox state.

Experiments to determine the flux through the membranes were carried out under a pressure of 0.03 kg/cm^2 using a microfiltration cell (Toyo Roshi UHP-25, Japan). The flux through the membranes was studied using distilled water, 0.1 M $Na_2S_2O_4$, and 0.01 M $(NH_4)_2Ce(NO_3)_6$ aqueous solutions. The flux was calculated from the volume of solution permeated per unit time and per unit area of the membrane surface. The data reported were averaged from measurements using at least five similar membranes, and the standard derivations were found within ±5%.

Results and Discussion

Composition of Viologen-Functionalized PVDF Membranes. The XPS N 1s and Cl 2p core-level spectra of the VBC-*g*-PVDF membrane after reacting with 4,4′-bipyridine (after reaction step I in Scheme 1) and the VBV-*g*-PVDF membrane (i.e., after reaction steps I and II in Scheme 1) are shown in Figure 2. The presence of the nitrogen signal is attributed to the introduced viologen groups since there is no nitrogen in PVDF or VBC. The N 1s core-level spectrum can be curve-fitted with three peak components. The peaks at 401.7, 399.5, and 398.6 eV are assigned to the positively charged nitrogen (N^+), the viologen radical cation ($N^\bullet$) formed during X-ray excitation of viologen dications in the XPS analysis chamber,[24] and the unreacted imine nitrogen (−N=) of the pyridine rings,[25] respectively. The [−N=]/total[N] ratio of 0.48 in Figure 2a suggests the successful monoquaternization of bipyridine after reaction step I. After further reaction with VBC (reaction step II) the amount of unreacted −N= is very small, and the dominant N^+ peak component in Figure 2b indicates that the 4,4′-bipyridine has been mostly diquaternized. The Cl 2p core-level spectrum (not shown) of VBC-*g*-PVDF membrane shows component peaks due to covalently bonded chloride (−Cl) only (a spin−orbit split doublet with binding energies for the Cl $2p_{3/2}$ and Cl $2p_{1/2}$ peak components at 200.2 and 201.7 eV, respectively), and no ionic chloride (Cl^-) signal is discernible. For the VBV-*g*-PVDF membrane, the Cl 2p core-level spectrum (Figure 2c) shows only the peak components (Cl $2p_{3/2}$ at 197.1 eV and Cl $2p_{1/2}$ at 198.6 eV) attributed to Cl^-, which implies that the grafted VBC groups have completely reacted with the 4,4′-bipyridine.

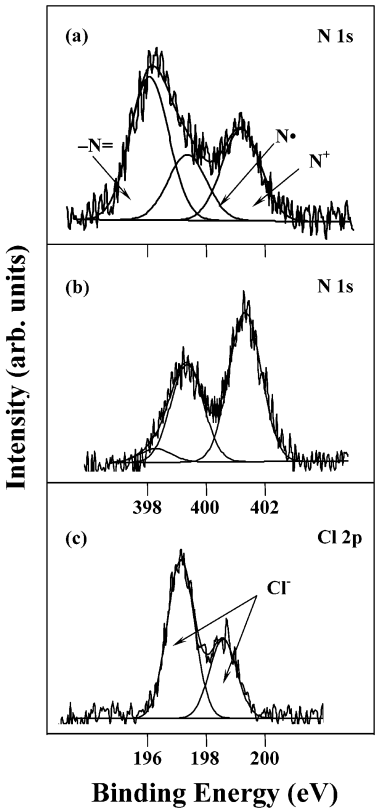

Figure 2. XPS N 1s core-level spectrum of (a) VBC-*g*-PVDF membrane after reaction with 4,4′-bipyridine (reaction step I in Scheme 1) and (b) N 1s and (c) Cl 2p core-level spectra of the VBV-*g*-PVDF membrane (after reaction steps I and II in Scheme 1).

Figure 3 shows the respective C 1s core-level spectra of the pristine PVDF and the VBV-*g*-PVDF membranes prepared using different [VBC]/[$-CH_2CF_2-$] feed ratios. In the case of pristine PVDF membrane (Figure 3a), the C 1s core-level spectrum can be curve-fitted with two peak components, with binding energies at 285.8 eV for the CH_2 species and 290.5 eV for the CF_2 species.[26] The ratio of these two peaks is about 1.05, which is in good agreement with the structure of PVDF and the data reported in the literature.[27] In the case of the VBV-*g*-PVDF membranes (Figure 3b−d), the C 1s core-level spectra were curve-fitted with three peak components. The component with binding energy at 284.6 eV is attributed to the hydrocarbon backbone of the grafted viologen-containing polymer chains. The PVDF main chains will contribute to the other two peak components (285.8 eV for the CH_2 and 290.5 eV for the CF_2 species). The CN species of the viologen moieties will also contribute to the component at 285.8 eV. The steady increase in the CH peak component intensity and the corresponding decrease in the CF_2 peak component intensity with increasing [VBC]/[$-CH_2CF_2-$] feed ratio indicates the increase in graft concentration of the VBV.

The VBV surface graft concentrations of the membranes can be derived from the carbon-to-fluorine ratio obtained from the XPS analysis. The graft concentration in terms of the number of VBV units per PVDF unit, or the $([VBV]/[-CH_2CF_2-])_{surface}$ molar ratio, can be obtained from the $([C]/[F])_{surface}$ ratio by taking into account the carbon stoichiometries of the graft and the main chains and the carbon-to-fluorine ratio of the PVDF main chains. Thus, the $([VBV]/[-CH_2CF_2-])_{surface}$

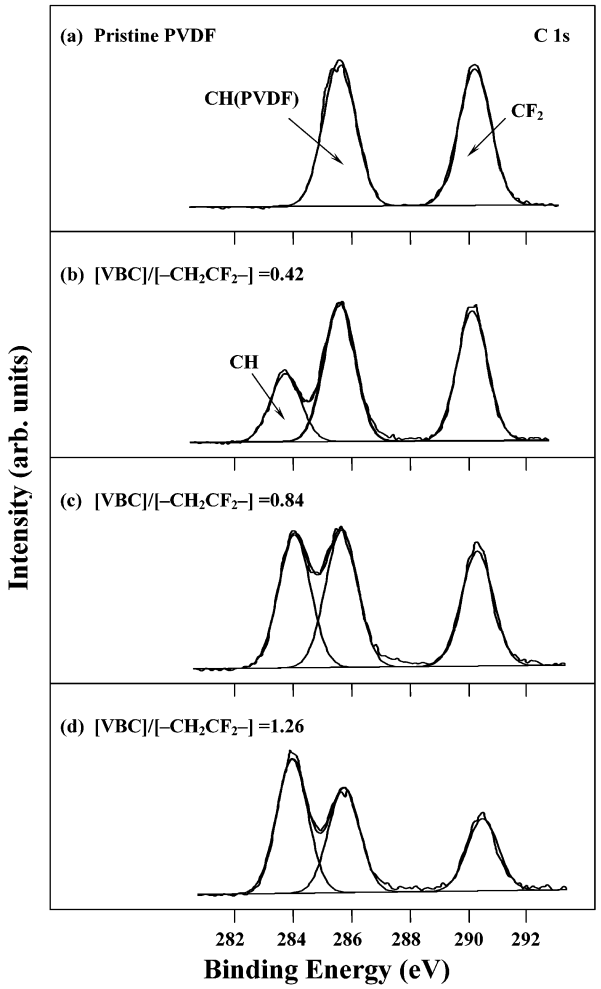

Figure 3. XPS C 1s core-level spectra of (a) pristine PVDF and the VBV-*g*-PVDF membranes prepared with [VBC] to [$-CH_2CF_2-$] molar feed ratio of (b) 0.42, (c) 0.84, and (d) 1.26.

molar ratio can be calculated from the following relationship:

$$([\text{VBV}]/[-CH_2CF_2-])_{\text{surface}} = (1/14)([\text{C}]-[\text{F}])_{\text{surface}}/[\text{F}]_{\text{surface}}$$

where the factor 1/14 accounts for the fact that there are 2 and 28 carbon atoms per repeat unit of PVDF and VBV, respectively. Similarly, the bulk VBV graft concentrations of the membranes, expressed as the $([\text{VBV}]/[-CH_2CF_2-])_{\text{bulk}}$ ratio, were determined from elemental analysis data and the carbon and fluorine stoichiometries of the graft and the main chains. Figure 4 shows the dependence of the surface and bulk graft concentration (expressed as either the ([C]/[F]) or ([VBV]/[$-CH_2CF_2-$]) molar ratio) on the [VBC] to [$-CH_2CF_2-$] feed molar ratio used for the thermally induced graft copolymerization. In Figure 4a, it can be seen that a low monomer feed ratio of 0.2 results in a $([\text{C}]/[\text{F}])_{\text{bulk}}$ ratio (1.15:1) which is only slightly higher than that of pristine PVDF (1:1). As the monomer feed ratio increases beyond 0.2, the surface and bulk graft concentrations of VBV increase significantly. The [VBC]/[$-CH_2CF_2-$] monomer feed ratio was restricted to less than 1.3 due to the dense formation of the VBC homopolymer at higher feed ratios. In general, the VBV graft concentration increases almost linearly with increasing [VBC]/[$-CH_2CF_2-$] molar feed ratio used for

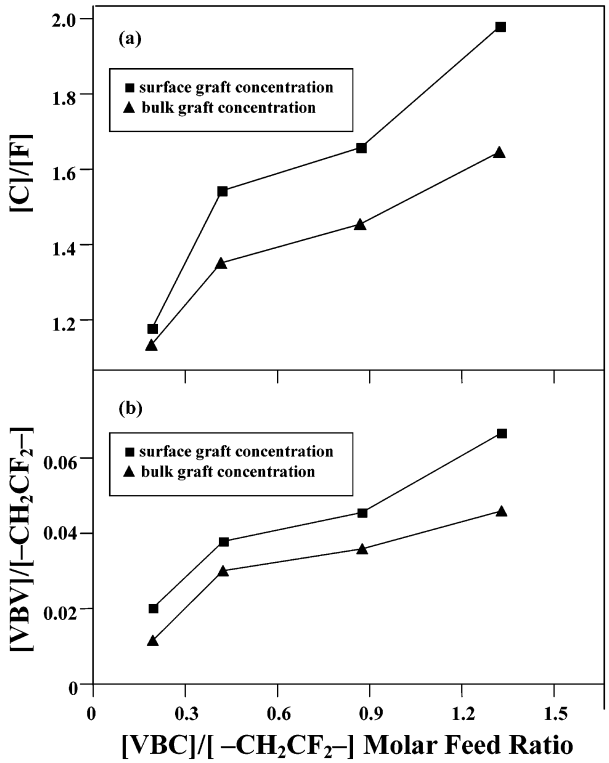

Figure 4. Effects of [VBC]/[$-CH_2CF_2-$] molar feed ratio on the surface and bulk VBV graft concentration in the terms of (a) [C]/[F] and (b) [VBV]/[$-CH_2CF_2-$] of the VBV-*g*-PVDF membranes.

the graft copolymerization, indicating that the monomer feed ratio is an important parameter which can be used to regulate the VBV graft concentration. From Figure 4, it can also be seen that the surface graft concentration of VBV is always higher than the corresponding bulk graft concentration. This is due to the immiscibility of the VBC polymer with the PVDF chains, the former being more hydrophilic than the latter. Surface enrichment of the hydrophilic component results in the copolymer membranes during the phase inversion process. As shown by the XPS results, all the surface-grafted VBC groups have reacted to give the viologen moieties. Hence, the data in Figure 4b shows that even with a high [VBC]/[$-CH_2CF_2-$] feed ratio, the extent of VBV surface grafting is less than 10 units in 100 $-CH_2CF_2-$ units. Nevertheless, this degree of grafting is sufficient to significantly alter the morphology and permeation properties of the membranes, as discussed below.

Surface Morphology and Pore Sizes of the MF Membranes. The scanning electron microscopy images of the bottom surface of pristine PVDF and MF membranes of different VBV graft concentrations are shown in Figure 5. The bottom surface of pristine PVDF membrane (Figure 5a) is smooth with very few pores. The VBV-*g*-PVDF membrane shown in Figure 5b has a bulk [VBV]/[$-CH_2CF_2-$] molar ratio of 0.029, and for this membrane, a fairly even distribution of pores on the bottom surface is obtained. With increasing VBV graft concentration, the membranes have a higher degree of porosity and larger pore size, as can be seen from Figure 5c,d.

The pore sizes of the various VBV-*g*-PVDF MF membranes were measured on a Coulter Porometer II apparatus using the commercial fluid Porofil as the wetting agent. The Porofil-wetted membranes were

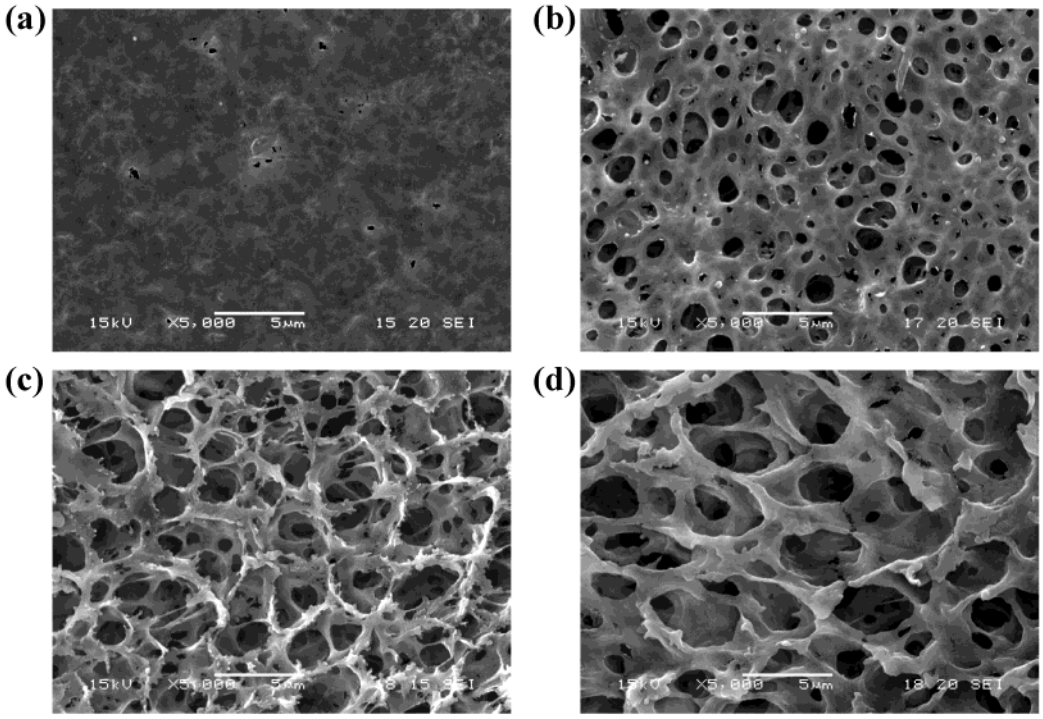

Figure 5. SEM images of the bottom surface of MF membranes: (a) pristine PVDF membrane; VBV-*g*-PVDF membranes of bulk [VBV]/[$-CH_2CF_2-$] molar ratio of (b) 0.029, (c) 0.035, and (d) 0.045.

Table 1. Pore Sizes and Permeation Rates through the Pristine PVDF and the VBV-*g*-PVDF MF Membranes

membrane	bulk [VBV]/[$-CH_2CF_2-$] molar ratio	max pore size[a] (μm)	min pore size[a] (μm)	mean pore size[a] (μm)	permeation rate R (10^{-6} cm s^{-1})		
					$R(V^{2+})$[b]	$R(V^{\bullet+})$[b]	$R(V^{\bullet+})/R(V^{2+})$
PVDF	0	1.36	0.27	0.59	1.2	1.2	1.0
VBV-*g*-PVDF	0.029	1.61	0.38	0.85	3.9	6.6	1.7
VBV-*g*-PVDF	0.035	1.95	0.37	1.23	4.5	16.2	3.6
VBV-*g*-PVDF	0.045	2.56	0.46	1.56	5.6	22.9	4.1

[a] These pore sizes were measured on the Coulter Porometer II which utilized a liquid displacement technique. [b] $R(V^{2+})$ and $R(V^{\bullet+})$ are the permeation rates of SSA through the MF membranes when the viologen moieties are in the oxidized and reduced form, respectively.

subjected to a pressure exerted by nitrogen. As the pressure increases to a point at which the nitrogen can overcome the surface tension of the liquid in the largest pores, the liquid will be pushed out from these pores. This pressure corresponds to the measurement of maximum pore size. With increasing pressure, the gas can flow through smaller pores until all the pores have been emptied. The range of pore size measurement is from 0.1 to 5.0 μm, corresponding to pressure ranging from 0.1 to 8.6 kg/cm^2. The relation between pore size and pressure is governed by the Washburn equation:[28] $Pr = 2\gamma \cos\theta$, where P is the pressure, r is the pore radius of the measured membrane sample, and $\gamma \cos\theta$ is the Wilhelmy surface tension. In each set of measurements, the pore size distribution, maximum pore size, minimum pore size, and mean pore size (which is based on the statistical evaluation of all pore sizes) were obtained. The pore sizes of the various MF membranes with different VBV graft concentrations are shown in Table 1. It can be seen that the mean pore size of the VBV-*g*-PVDF membrane is bigger than that of the pristine PVDF membrane, and the pore size increases with increasing VBV graft concentration. While this trend is consistent with the SEM images in Figure 5, the difference in pore size as reflected by the SEM images is more drastic than that shown in Table 1. To understand this apparent anomaly, the structural compositions of the membranes need to be considered.

The top surfaces of the MF membranes are less porous and are significantly rougher than the bottom surfaces. Since the top and bottom surfaces are so different, there must be a transition region in between. Hence, the cross sections of the MF membranes were also investigated by SEM. In the cross sections of membranes prepared from PVDF solutions in NMP (Figure 6a), an important feature is the presence of cavities (ii) between the thin dense top layer (i) and the thicker microporous bottom layer (iii). In the membrane casting process, as the casting solution is immersed in the water bath, the hydrophobic PVDF chains aggregate immediately at the interface. Amorphous PVDF tends to precipitate at these sites, thus developing the dense skin layer. Once the surface layer is formed, access of the nonsolvent to the remaining matrix is restricted. As drops of the nonsolvent (water) swell with solvent (NMP) absorbed from the surroundings, a thin layer of gelled polymer surrounding them eventually becomes the wall of the alveoli. The ultimate size of the alveoli in the substructure depends on the rate at which solidification occurs. The cavity layer is thus associated with the faster solvent/nonsolvent exchange, while the microporous bottom layer is due to slower solidification. In the case of the VBV-*g*-PVDF membrane (Figure 6b), a similar three-layer structure was found. When the VBV graft concentration of VBV-*g*-PVDF membranes increases, the cavity layer becomes thicker and the

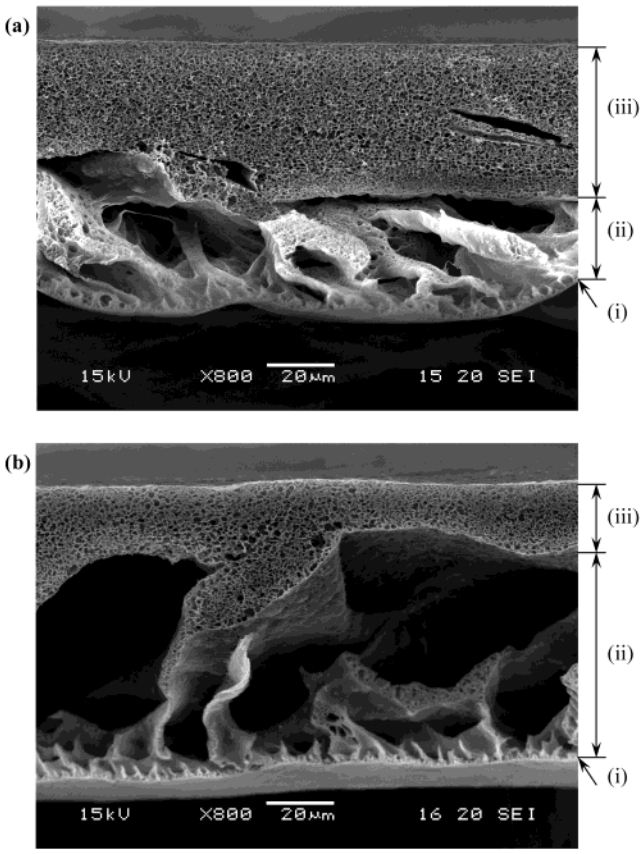

Figure 6. SEM images of the cross section of (a) the pristine PVDF membrane and (b) VBV-*g*-PVDF membrane of bulk [VBV]/[$-CH_2CF_2-$] molar ratio of 0.035: (i) top skin layer, (ii) cavity layer, and (iii) bottom microporous layer.

microporous bottom layer ((iii) in Figure 6b) becomes thinner, leading to a larger mean pore size. As the mean pore size is a statistical calculation based on the pore size distribution, it is highly dependent on the changes in the internal structural composition of the membrane.

Permeability Properties of the MF Membranes. The permeability experiments were conducted with the viologen moieties in either the oxidized or reduced state. When the VBV-*g*-PVDF membrane was treated with the 0.1 M $Na_2S_2O_4$ solution, it turned immediately from pale yellow to dark blue, which is an indication of the reduction of the grafted viologen from the dicationic V^{2+} state to the radical cationic $V^{\bullet+}$ state. The dark blue color was maintained for up to 5 min when the membrane was immersed in water, and the color bleached slowly after that due to the oxidation of the $V^{\bullet+}$ by dissolved oxygen in the water. To ensure that the redox state was maintained during the permeability experiment, the permeability experiment was conducted for 3 min with the membrane in the reduced state. The viologen was oxidized back to the dicationic state by treatment with 0.01 M $(NH_4)_2Ce(NO_3)_6$ solution, and the permeability experiment was repeated for 3 min. These experiments were conducted for a number of cycles.

Figure 7 shows the reversible changes in the permeation rates of the SSA after the redox state of the viologen moieties in the VBV-*g*-PVDF membranes was changed by treatment with either the reducing or oxidizing agent. The permeation rate shown in Figure 7 for each 3 min interval is the average value calculated for that interval. The permeation rate R (cm/s) is calculated from the following equation: $R = kV/AC$, where k (M/s) is the efflux (change in SSA concentration

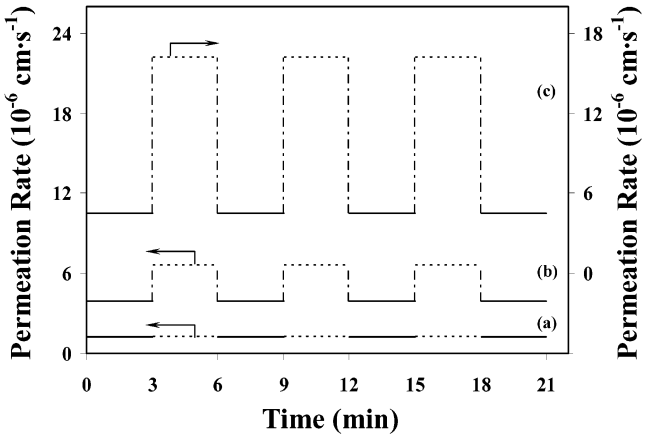

Figure 7. SSA permeation rates through MF membranes at 25 °C: (a) pristine PVDF membrane; VBV-*g*-PVDF membranes of bulk [VBV]/[$-CH_2CF_2-$] molar ratio of (b) 0.029 and (c) 0.035. The dotted line (···) and full line (—) indicate the permeation rate through the membrane with the viologen moieties in the reduced and oxidized state, respectively.

of outer aqueous solution in unit time), A (cm^2) is the surface area of MF membrane, and V (cm^3) is the volume of the outer aqueous phase. C (M) denotes the concentration of SSA in the inner aqueous phase. After the series of permeability experiments, the absorbance of SSA in the inner aqueous phase of the cell was measured to get the value of C. It was found to be $(0.98 \pm 0.01) \times 10^{-2}$ M, which was nearly equal to the initial SSA concentration (10^{-2} M). Hence, C can be assumed to be constant for the duration of the experiment. In the case of pristine PVDF membrane (Figure 7a), its permeation rate after treatment with either the reducing or oxidizing agent is not changed. On the other hand, the permeability of the VBV-*g*-PVDF membranes depends on the redox state of the viologen. When the reduced membrane was used in the cell, the permeability of the SSA was enhanced, as shown by the abrupt increase in the permeation rate in Figure 7b. After the VBV-*g*-PVDF membrane was reoxidized, the permeability of this membrane decreased to the level before reduction occurred, as shown in Figure 7b. The extent of change in the permeability of the VBV-*g*-PVDF membrane with changes in its redox state is dependent on the VBV graft concentration. The membrane used in Figure 7b had a bulk [VBV]/[$-CH_2CF_2-$] molar ratio of 0.029, whereas the data in Figure 7c were obtained with a membrane with a bulk [VBV]/[$-CH_2CF_2-$] molar ratio of 0.035. The effects of the VBV graft concentration of the VBV-*g*-PVDF membrane on the redox-sensitive permeation rates are summarized in Table 1.

The observed change in the permeability of the VBV-*g*-PVDF membrane with changes in the redox state of the viologen can be explained by considering the conformation of the viologen side chains. Normally, viologen in the dication state is highly soluble in water, but its solubility decreases in the reduced radical cation state.[20] In the VBV-*g*-PVDF membrane, when the grafted viologen containing polymer is in its oxidized form, the polymer chains may be repelled by the charges on the dicationic side chains and extend more into the pores. When the grafted viologen containing polymer is changed to its reduced form, the hydrophobic radical cationic chains may be in a more entangled or collapsed state, leading to reduced spatial resistance. The effective pore size may become bigger, and the permeants would pass through more easily. However, the permeability of ions through the pores is dependent not only on the effective

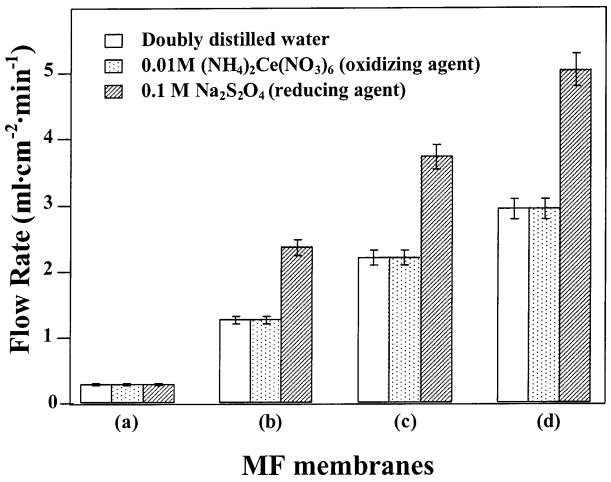

Figure 8. Flux of aqueous solutions through (a) the pristine PVDF membrane; VBV-*g*-PVDF membranes of bulk [VBV]/[$-CH_2CF_2-$] molar ratio of (b) 0.029, (c) 0.035, and (d) 0.045.

pose size but on the electric charge of the pores as well.[29] The reduced form of the viologen polymer is less positively charged, which may allow the SSA anions to move through the pores more effectively, hence increasing its permeability. Since electrostatic repulsion/attraction is a common retarding force against the concentration difference driving force when ionic permeants are used in a positively/negatively charged membrane, some studies have used nonionic permeants instead.[15] In the present study, a second series of experiments using an external pressure as the driving force were carried out to minimize the electrostatic phenomenon.

The second series of experiments to illustrate redox-sensitive permeation was undertaken by measuring the flux of doubly distilled water, 0.1 M $Na_2S_2O_4$, and 0.01 M $(NH_4)_2Ce(NO_3)_6$ aqueous solutions through the different MF membranes under an external pressure. As shown in Figure 8, the flux of any particular solution is the lowest through the pristine PVDF membrane, and the flux increases as the VBV graft concentration in the membrane increases. This is consistent with the increase in pore size as described earlier. For each MF membrane, the flux of the doubly distilled water and oxidizing aqueous solution are also the same. This suggests that the electrostatic repulsion between the polymer chains and the ionic permeant is not a dominant factor in these experiments, and the differences in flux of these solutions through the different VBV-*g*-PVDF membranes are determined by the pore size. However, the flux of the aqueous reducing solution though VBV-*g*-PVDF membranes is clearly larger than those of the oxidizing solution and water. The result again confirms the effect of the redox state of the viologen on the effective pore size, and the VBV-*g*-PVDF membrane can be viewed as a redox-sensitive valve. Since the redox states of viologen can also be changed photochemically and electrochemically, the applications of such kinds of viologen-functionalized membranes will be studied in greater details in the future.

Conclusion

A new viologen-containing microfiltration membrane (VBV-*g*-PVDF) was successfully prepared. The molecular graft copolymerization of VBC with ozone-pretreated PVDF in NMP was first carried out followed by the casting of the copolymer into a microfiltration membrane by the phase inversion method. Viologen moieties (VBV) were then introduced by the reaction of 4,4′-bipyridine with the grafted VBC. Diquaternization of the bipyridine was achieved by a subsequent reaction with VBC. The surface graft concentration of the viologen in the membrane can be regulated by the VBC monomer concentration used in the initial graft copolymerization process. The mean pore size of the MF membranes increases with increasing VBV graft concentration. The permeation rate and flux through the VBV-*g*-PVDF membrane can be reversibly controlled by means of changing the redox state of the viologen. The present study has shown that molecular functionalization is a relatively effective approach for the preparation of membranes with well-controlled pore size and redox-sensitive properties, and such membranes have the potential for applications as redox gates and in controlled chemical release.

References and Notes

(1) Mulder, M. *Basic Principles of Membrane Technology*; Kluwer Academic Publishers: Dordrecht, 1996.
(2) Messing, R. A. *Immobilized Enzymes for Industrial Reactors*; Academic Press: New York, 1975.
(3) Doretti, L.; Gattolin, P.; Burla, A.; Ferrara, D.; Lora, S.; Palma, G. *Appl. Biochem. Biotechnol.* **1998**, *74*, 1−12.
(4) Pasquali, C.; Fialka, I.; Huber, L. A. *Electrophoresis* **1997**, *18*, 2573−2581.
(5) Lee, Y. M.; Shim, J. K. *J. Appl. Polym. Sci.* **1996**, *61*, 1245−1250.
(6) Wang, P.; Tan, K. L.; Kang, E. T.; Neoh, K. G. *J. Membr. Sci.* **2002**, *195*, 103−114.
(7) Chen, N. P.; Hong, L. *Polymer* **2002**, *43*, 1429−1436.
(8) Porte-Durrieu, M. C.; Aymes-Chodur, C.; Betz, N.; Baquey, C. *J. Biomed. Mater. Res.* **2000**, *52*, 119−127.
(9) Huang, R. Y. M.; Pal, R.; Moon, G. Y. *J. Membr. Sci.* **2000**, *167*, 275−289.
(10) Han, S.; Choi, W. K.; Yoon, K. H.; Koh, S. K. *J. Appl. Polym. Sci.* **1999**, *72*, 41−47.
(11) Müller, M.; Oehr, C. *Surf. Coat. Technol.* **1999**, *119*, 802−807.
(12) Tarvainen, T.; Nevalainen, T.; Sundell, A.; Svarfvar, B.; Hyrsyla, J.; Paronen, P.; Jarvinen, K. *J. Controlled Release* **2000**, *66*, 19−26.
(13) Fan, L. H.; Harris, J. L.; Roddick, F. A.; Booker, N. A. *Water Res.* **2001**, *35*, 4455−4463.
(14) Hietala, S.; Maunu, S. L.; Sundholm, F. *Macromolecules* **1999**, *32*, 788−791.
(15) Okahata, Y.; Ariga, K.; Seki, T. *J. Chem. Soc., Chem. Commun.* **1986**, 73−75.
(16) Cosnier, S.; Innocent, C.; Moutet, J. C.; Tennah, F. *J. Electroanal. Chem.* **1994**, *375*, 233−241.
(17) Brink, L. E. S.; Elbers, S. J. G.; Robbertsen, T.; Both, P. *J. Membr. Sci.* **1993**, *76*, 281−291.
(18) Svarfvar, B. L.; Ekman, K. B.; Sundell, M. J.; Näsman, J. H. *Polym. Adv. Technol.* **1996**, *7*, 839−846.
(19) Iwata, H.; Hirata, I.; Ikada, Y. *Macromolecules* **1998**, *31*, 3671−3678.
(20) Monk, P. M. S. *The Viologens: Physicochemical Properties, Synthesis and Applications of the Salts of 4,4′-Bipyridine*; John Wiley & Sons Ltd.: Chichester, 1998.
(21) Okahata, Y.; Enna, G. *J. Phys. Chem.* **1988**, *92*, 4546−4551.
(22) Ying, L.; Wang, P.; Kang, E. T.; Neoh, K. G. *Macromolecules* **2002**, *35*, 673−679.
(23) Walton, H. F. *Principles and Methods of Chemical Analysis*, 2nd ed.; Prentice Hall: Englewood Cliffs, NJ, 1964; p 175.
(24) Alvaro, M.; Garcia, H.; Garcia, S. Marquez, F.; Scaiano, J. C. *J. Phys. Chem. B* **1997**, *101*, 3043−3051.
(25) Camalli, M.; Caruso, F.; Mattogno, G. *Inorg. Chim. Acta* **1990**, *170*, 225−231.
(26) Briggs, D. *Surface Analysis of Polymers by XPS and Static SIMS*; Cambridge University Press: New York, 1998.
(27) Beamson, G.; Briggs, D. *High-Resolution XPS Organic Polymers: The Sienta ESCA Database*; John Wiley: New York, 1992.
(28) Washburn, E. W. *Proc. Natl. Acad. Sci. U.S.A.* **1921**, *7*, 115.
(29) Rautenbach, R.; Albrecht, R. *Membrane Processes*; John Wiley & Sons Ltd.: Chichester, 1989.

MA034794O